STUDY ON SEISMIC PERFORMANCE OF NEW PRECAST POST-TENSIONED BEAM-COLUMN CONNECTION (PART 2)

TS. **ĐỖ TIẾN THỊNH**
Viện KHCN Xây dựng
Assoc.Prof.Dr. **KUSUNOKI KOICHI**
Đại học Tokyo
Prof. **TASAI AKIRA**
Yokohama National University, Japan

Tóm tắt: *Bài báo này trình bày kết quả nghiên cứu của 3 mẫu thí nghiệm liên kết dầm – cột biên bê tông cốt thép lắp ghép ứng lực trước được thí nghiệm tại Phòng Thí nghiệm Kết cấu của Đại học Quốc gia Yokohama, Nhật Bản. Mục đích của thí nghiệm nhằm kiểm chứng khả năng chịu động đất của loại liên kết này. Kết quả thí nghiệm cho thấy liên kết dầm - cột không có khóa chống cắt có độ trượt tương đối giữa dầm và cột và biến dạng dư lớn. Các mô hình thí nghiệm có khóa chống cắt có ứng xử rất tốt với biến dạng dư nhỏ, dầm gần như không bị trượt so với cột, hư hỏng của các cấu kiện dầm và cột rất ít, khả năng chịu lực tốt.*

Từ khóa: *Khóa chống cắt, ứng lực trước không bám dính, bê tông lắp ghép, liên kết dầm – cột.*

Abstract: *This paper presents experimental results of three precast prestressed concrete beam-column connection specimens which were tested at Structural Laboratory of Yokohama National University, Japan. The aim of the experiment is to prove seismic behavior of this type of connection. The experimental results show that the beam-column connection without shear key has large slip and residual deformation. The beam-column connections with shear key have good seismic behavior with small residual deformation, minor damage of beam and column, and nearly no slip between beam and column.*

Keywords: *shear key, unbonded presstressed, precast concrete, beam-column connection***.**

1. Introduction

From the experimental results of the specimens in the Phase 1[1, 2], it can be seen that the unbonded post-tensioned precast concrete connection with shear bracket has high possibility to apply for long-span office buildings. However, there were still some undesirable behaviour of the specimens such as crush of concrete at the upper part of the beam, damage of the top of the shear bracket and the beam socket. The aim of this study, named Phase 2, is to improve the design of the connection in the Phase 1 to obtain enhanced performance and avoid unexpected failure modes. Moreover, shear friction at the beam to column interface was also investigated. This type of structure has advantages such as over large span, good seismic performance with minimum damage for beam and column elements, reusable like steel structure. This type of structure has high ability to apply in high seismicity like Japan as well as in low to moderate seismicity area like Viet Nam. .

2. Test program

2.1 Test specimens

There are three specimens named SB-A, SF-A, and SB-LA. These specimens corresponded to the specimens SB, SF, and SB-L in the Phase 1[1]. The specimen with slab and spandrel beam was not included in this study. Brief outline and specification of the specimens is shown in Table 1, and reinforcement detail is shown in Figure 1**.** Shear strength of the bracket and the volume of PC bars were determined in the same way as in the Phase 1[1]. Consequently, the shear resistant area of the bracket and volume of the PC bars of the specimens in the Phase 2 were identical with those of specimens in the Phase 1.

Table 1. *Specimens outline*

Specimens		SB-A	SF-A	SB-LA
Beam	Section (mm^2)	300 x 500		
	F_c (N/mm^2)	69.9	60.4	68.6
	f_y (N/mm^2)	339.1	339.1	339.1
	f_{wy} (N/mm^2)	313.1	313.1	313.1
	PC bars	2- ϕ15 Grade C	2- ϕ 26 Grade A	2- ϕ 15 Grade C
	σ_0 (N/mm^2)	1.83	4.02	1.83
	P_0/P_y	0.72	0.72	0.72
	PC length (mm)	1500	1500	1500
Column	Section (mm^2)	400 x 400		
	F_c (N/mm^2)	69.9	60.4	68.6
	f_y (N/mm^2)	534.4	534.4	534.4
	f_{wy} (N/mm^2)	313.1	313.1	313.1
Bracket	a_w (mm^2)	3036	-	4950
	Length L (mm)	50	-	50

Where: F_c : concrete compressive strength, f_y : yield strength of main reinforcement, f_{wy} : yield strength of lateral reinforcement, σ_0 : initial beam compressive stress, P_0 : initinal prestressed load, P_y : PC bar yield load, a_w : shear resistant area.

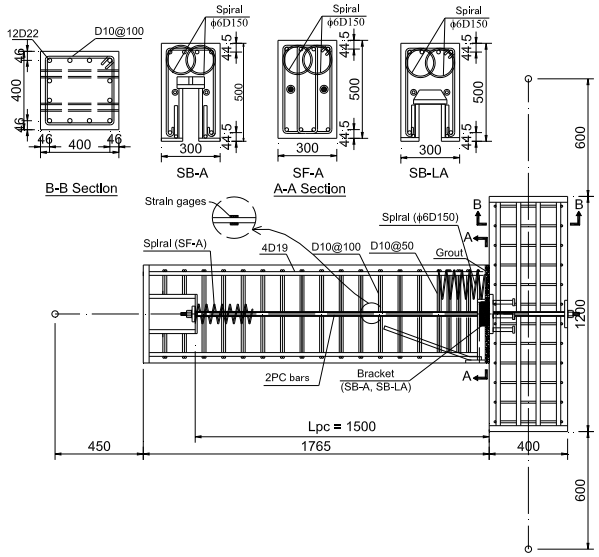

Figure 1. *Reinforcement details of the specimens*

As seen from the test result of the specimens in the Phase 1, the top of the bracket was deformed after the test, caused by large concentrated stress. Therefore, in the Phase 2, the shear bracket was designed so that the stress at its top face does not exceed the yield strength of the steel:

$$\sigma_u = \frac{Q_u}{A} \le \sigma_y \quad (1)$$

where:

Q_u: ultimate shear force at the beam end (N);

σ_y: yield strength of the steel (N/mm^2);

A: effective area of the top face of the bracket (mm^2), $A = b.l_e$, where b was the width of the bracket (mm), and l_e was the effective length of the bracket which contacted to the beam socket (mm).

The width and effective length of the bracket are shown in Figure 2. Total length of the bracket was 50

mm from the column face. The gap between the beam and the column filled with mortar was 20mm. Hence the effective length l_e is 30mm.

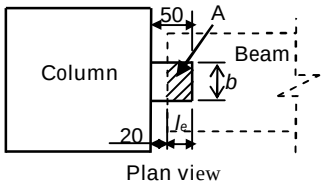

Figure 2. *Effective area of the top face of the bracket*

In order to satisfy Eq. (1), the shape of shear bracket was redesigned as T-shaped with wide top horizontal plate to enlarge the effective area. The widths of top plates were 80mm and 110mm for specimens SB-A and SB-LA, respectively.

For the U-shaped steel box, beside the design formulas used in Phase 1[(1)], the top horizontal plate of the steel box should be designed for bending moment, caused by the reaction force from the shear bracket. In order to limit flexural deformation, maximum tensile stress at the top face of the horizontal plate should not exceed the yield strength of the steel:

$$\sigma_u \leq \sigma_y \qquad (2)$$

Where:

σ_u: maximum tensile stress at the midpoint of upper face of the top plate (N/mm^2);

σ_y: yield strength of the material (N/mm^2).

In order to satisfy Eq. (2), thicker plate (t=25mm) and strengthen plates was used at the top of the steel box. Photos of the shear bracket and U-shaped steel box are shown in Figure 3.

SB-A SB-LA

Figure 3. *Shear bracket and U-shaped steel box*

Test results of the specimens in the Phase 1 showed that the upper part of the beam near the column face was severely crushed. In order to prevent this damage, two ϕ6-D150 interlock steel spirals were used at the top corner of the beam to confine the concrete.

2.2 Test setup and loading history

The experimental setup is shown in Figure 4. The lower end of the column was connected to the reacting floor by the pin while the upper end was connected to the reaction wall by horizontal two-end pin brace that is equivalent to a vertical roller. The cyclic load was applied to the beam end by the 1000 kN hydraulic jack that attached to the beam end with the pin. The gravity load was applied to the beam as a concentrated vertical load at the distance of 215 mm from the column face.

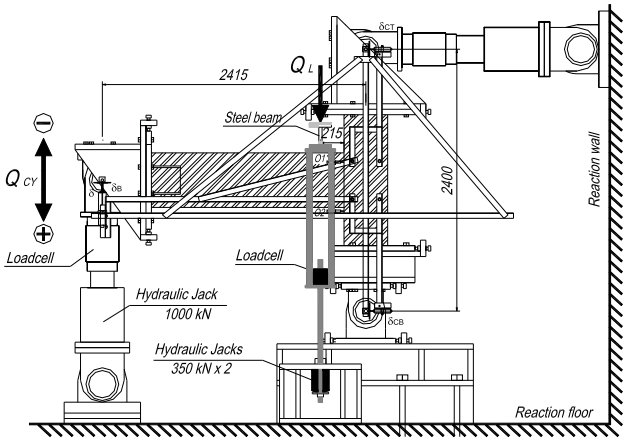

Figure 4. *Test setup*

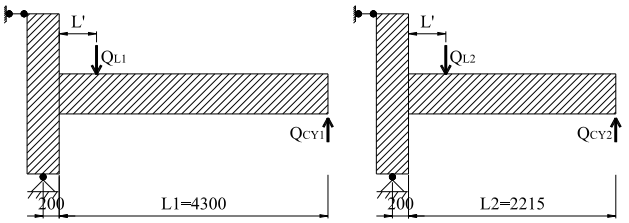

a) Prototype model b) Actual specimen

Figure 5. *Illustration of the terms in the Equation (3)*

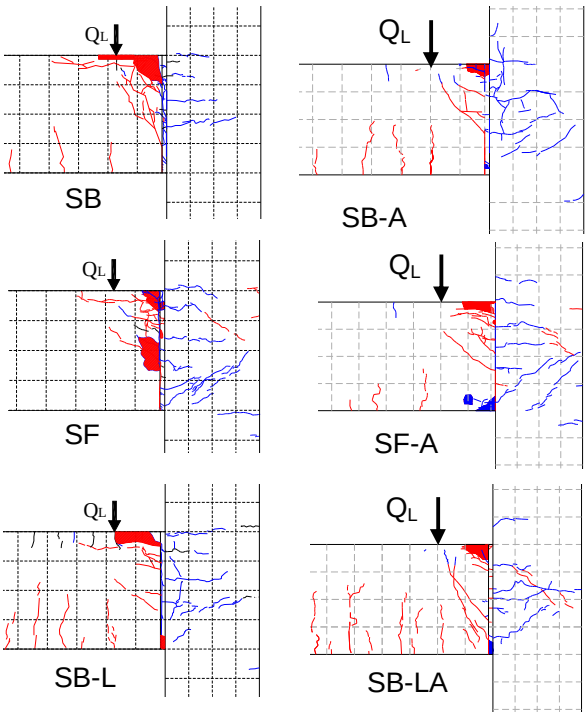

a) Phase 1 specimens[1] b) Phase 2 specimens

Figure 6. *Crack patterns of specimens at 4% drift angle*

The specimens were tested under simultaneous action of cyclic and gravity load. First, the gravity load was applied gradually to designated value, and then the cyclic load was applied. As mentioned before, the beams of the specimens were shortened from 4.3m to 2.215m, hence, in order to generate the same combination of moment and shear force at the beam column interface as in original condition; the gravity load was controlled according to the original gravity load Q_{L1} and the cyclic load Q_{CY} as:

$$Q_L = Q_{L1} + \left(\frac{L_2 - L_1}{L_1 - L'}\right) Q_{CY} \qquad (3)$$

Where: Q_{L1} was the original gravity load, L_1 was the original beam length, L_1 = 4.3m, L_2 was the new beam length, L_2 = 2.215m, the beam length was considered up to column face, L' was the distance from the gravity load to the column face, L' = 0.215 m, Q_{CY} was the cyclic load. Q_{CY} has the same sign with Q_L if they act on the same direction, and vice versa. These terms are shown in Figure 5.

3. Test results and discussions

3.1 Visual Observation

Figure 6 shows the crack patterns of the specimens of Phase 1 [1] and Phase 2 at 4% drift angle. Much fewer cracks were observed in all specimens, compared to those of specimens in the Phase 1. Crush of concrete at the top of the beam near the column face was significantly diminished compared to specimens in the Phase 1, proving the effectiveness of the spiral steels.

The bracket and beam socket after the test were shown in Figure 7. As seen in this figure, the shear bracket and beam socket were not suffered from any damage, although they experienced very large vertical load and high drift level. Especially in specimen SB-LA where the gravity load was 1.5 times larger than that in other specimens. Furthermore, in case of specimens with shear bracket, it was effortless to separate the beam out of the column after the test, confirmed the disassemble capability of this type of structure. Eq. 1 satisfied to prevent the bracket from deformation.

SB-A SB-LA

Figure 7. *Shear bracket and beam socket after tested*

3.2 Hysteresis behavior

The hysteresis characteristics of the specimens are shown in Figure 8 as the relationship between moment and drift angle. The superimposed dashed lines on this figure illustrate the hysteresis behavior and modeled as tri-linear skeleton curve. The moment and rotation angle at the limit states were determined as follow[6]:

Decompression occur state:

$$M_s = \frac{1}{2}\left(1-\frac{\eta_e}{0.85}\right)\eta_e BD^2\sigma_B \quad (4)$$

$$R_s = \frac{M_s}{3EIL} \quad (5)$$

Yield limit state:

$$M_y = \frac{1}{2}\left(1-\frac{\eta_y}{0.85}\right)\eta_y BD^2\sigma_B \quad (6)$$

$$R_y = \frac{\Delta\varepsilon_{PC}}{0.5D}L_{PC} + \frac{M_y}{3EIL}, \Delta\varepsilon_{PC} = \varepsilon_{py} - \varepsilon_{pe} \quad (7)$$

Ultimate limit state, $M_u = M_y$.

$$R_u = \frac{\Delta\varepsilon_{PC}}{0.5D}L_{PC} + \frac{M_y}{3EIL}, \Delta\varepsilon_{PC} = \varepsilon_{pu} - \varepsilon_{pe} \quad (8)$$

where:

η_e: = $P_e/BD\sigma_B$;

P_e: initial prestress force (N);

B, D: width and height of the beam (mm);

σ_B: concrete compressive strength (N/mm^2);

η_y: = $P_y/BD\ \sigma_B$;

P_y: PC bars yield force (N);

L_{PC}: PC length (mm);

E: Young modulus of the concrete (N/mm^2);

I: second moment of the beam section (mm^4);

L: beam length (mm);

ε_{pe}: initial PC strain ($\mu\varepsilon$);

ε_{py}: PC strain at yielding ($\mu\varepsilon$);

ε_{pu}: PC strain at ultimate state ($\mu\varepsilon$).

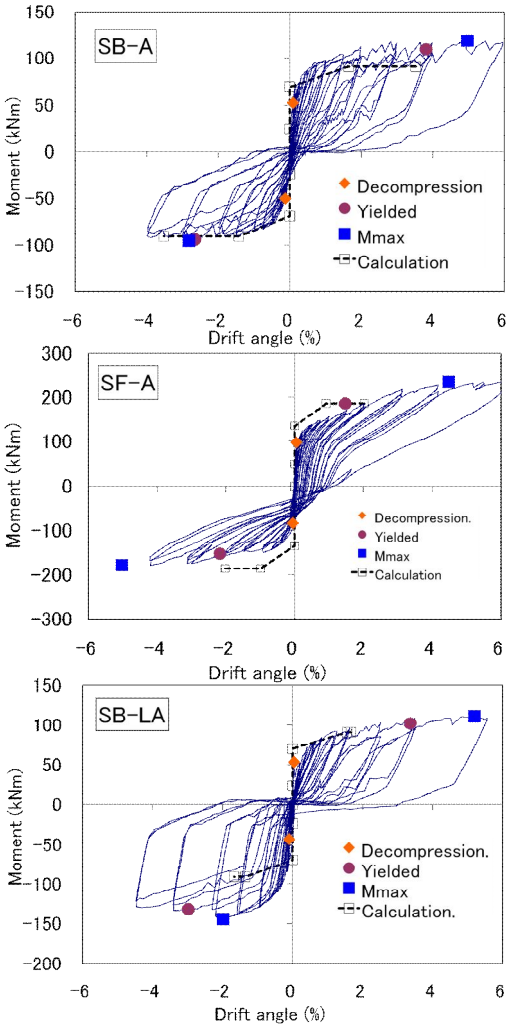

Figure 8. *Moment – drift angle relationship*

Table 2. *Summarized test results*

Specimens	Loading Direction	M_d (kNm)	R_d (%)	M_y (kNm)	R_y (%)	M_{max} (kNm)	R_{max} (%)	M_y/M_{ycal}
SB-A	+	52.7	0.09	109.4	3.82	118.7	4.97	**1.3**
	–	-50.3	-0.12	-94.2	-2.65	-95.4	-2.82	**1.1**
SF-A	+	97.1	0.09	185.6	1.99	234.9	5.21	**0.99**
	–	-84.7	-0.2	-152.5	-1.74	-178.7	-4	**0.81**
SB-LA	+	53.8	0.07	101.9	3.85	110.9	5.62	**1.2**
	–	-43.1	-0.15	-132	-2.61	-144.3	-1.82	**1.5**

Where: M_d, R_d : moment and story drift when opening occurred; M_y, R_y : moment and story drift at yielding; M_{max} , R_{max} : maximum moment and corresponded story drift; M_{ycal}: calculated yielded moment strength;

All the specimens were successfully passed the drift of 4% in negative directions and 6% in positive direction. No fracture of PC bars was recorded. As seen in **Figure 8**, while the self-centering characteristics of the specimens SB-A and SB-LA were very good, that of specimen SF-A was poor. In the specimens with shear bracket, yield moment strength well exceeded the modeled values. Average experimental yield moments were 20% and 35% larger than the calculated ones for specimens SB-A and SB-LA, respectively. In the specimen without shear bracket (SF-A), while the strength in the positive direction was almost the same with the modeled one, it was 80% of the modeled value in the negative direction. As illustrated in the **Figure 9**, when the beam slip occurs, the moment lever arm in negative direction was shorter than that in positive direction, made the flexural strength in negative direction smaller than that in the positive direction. It can be said that in the connection without bracket, under the effect of beam slip, it was difficult to predict the flexural strength of the connection. This was one of the disadvantage of the connection without shear bracket.

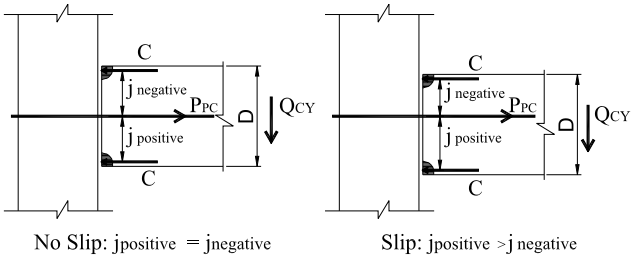

Figure 9. *Illustration of moment strength*

3.3 Beam Slip and Friction Coefficient

Figure 10 shows the relationship between the gravity load and quantity of beam slip at the beginning of the test (before applying of the cyclic load). The gravity load was applied monolithically up to 255 kN (SB-A and SF-A) and 382 kN (SB-LA). Up to gravity load of 255 kN, the amount of slip was mostly the same for all specimens, whether with or without shear bracket. It can be said that shear bracket did not contribute to the shear strength of the connection at this stage. For specimen SB-LA, when the gravity load exceeded 255 kN, the amount of beam slip significantly increased, expressed that the slip started to occur.

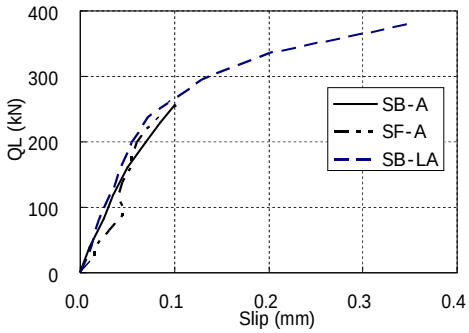

Figure 10. *Beam slip – gravity load relationship*

The beam slip – drift angle relationships of three specimens are shown in **Figure 11**. It can be seen that the beam slip of specimen without shear bracket (SF-A) was almost the same with that of specimen SF in the Phase 1, excessive larger than that of the specimens with shear bracket (SB-A and SB-LA). From the test result, it concluded that the shear bracket successfully prevented the slip of the beam. **Figure 12** shows the beam slip and the Q_B/P_{PC} ratio relationship of the specimen SF-A. The dashed line expresses the upper bound of the ratio of each loading cycle and illustrates the friction coefficient μ. It can be seen that, beam slip occurred when the value of μ was around 0.45.

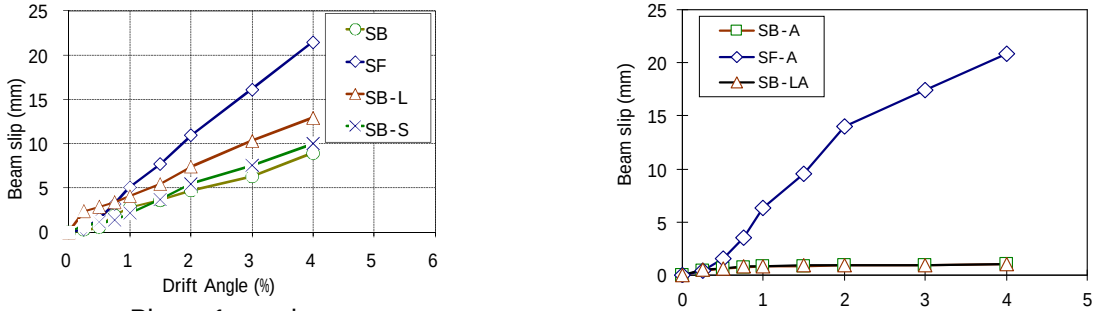

Figure 11. *Beam slip – drift angle relationship of all specimens*

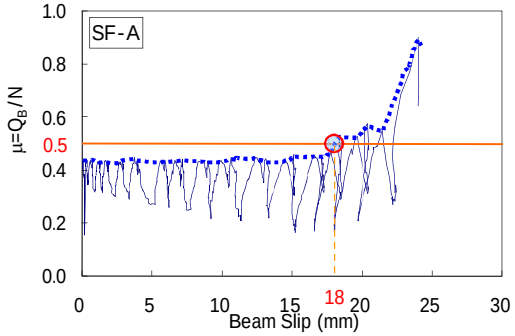

Q_B : Beam shear force; N : PC force

Figure 12. *Beam slip – friction coefficient relationship, SF-A*

3.4 Contribution of shear bracket and shear friction to the shear strength of the connection

Figure 13 shows the locations of strain gages pasted on the U-shaped steel box and the observed strains of the specimens SB-A and SB-LA. Strain gages were attached at the top horizontal plate and vertical plates of the steel box. For the specimen SB-A, strain gages were attached at middle and upper part of the vertical plates to confirm whether the strain varied along the plate or not. It can be seen from the **Figure 13** that the strains did not vary along the height of the vertical plates. From 2% drift angle, strains in these plates became stable. Maximum strains of the top horizontal plate in both specimens were 0.12%, about 50% of the yield strain. This improved that Eq. 2 was safe to design the steel box.

The tensile force in vertical plates of the steel box was calculated as follow: $T = E \cdot \varepsilon \cdot a$ (10)

where:

E: Young modulus of the steel (N/mm^2);

ε : strain ($\mu\varepsilon$);

a: total sectional area of vertical plates (mm^2).

In Figure 14, Q_b was the shear force resisted by the shear bracket. It can be seen that the reaction force from the bracket was resisted by vertical plates and transferred to bottom part of the beam. Therefore, it can be considered that the tensile force T in vertical plates of the steel box corresponded to the actual shear force transfer by the bracket.

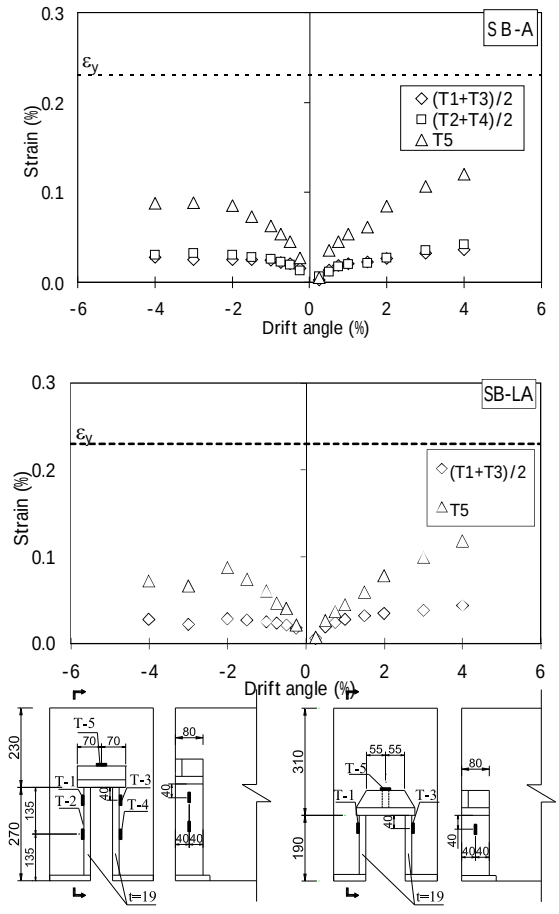

Figure 13. *Strain of the U-shaped steel box*

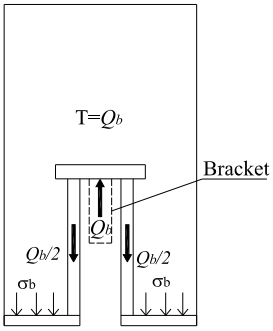

Figure 14. *Transfer of shear force from bracket to beam*

As proposed in reference (3), shear strength of the bracket was designed by the equation:

$$Q_s = 0.9\frac{F_y}{1.5\sqrt{3}}a_w \geq Q_L \quad (9)$$

where: Q_s is the shear strength of the bracket, F_y is the yield strength of the steel plate, a_w is the vertical shear resistance area, and Q_L is the shear force at the beam end induced by the gravity load.

In this study, SN490C steel was used, F_y = 325 N/mm^2. Shear resistance area a_w were 3036 and 4950 mm^2, for specimens SB-A and SB-LA, respectively. The value of shear strength Q_s were 342 kN and 557.3 kN for specimens for specimens SB-A and SB-LA, respectively.

Table 2 shows the ratio of tensile force T and gravity load QL. It can be seen that at small drift angle, most of the shear force was resisted by shear friction (77% and 78% at 0.5% drift angle, for specimen SB-A and SB-LA, respectively). When drift angle increased, contribution of shear bracket increased (62% and 65% at 4% drift angle and neutral position). Moreover, at peak drift position, this contribution was less than that at neutral position.

Table 3. *Shear resistance of the bracket*

Specimen	Drift angle (%)	Tensile force T (kN)	Shear strength of bracket Q_s (kN)	T/Q_s
SB-A	0.5%	74.5	342.0	**0.22**
	1%	121.5	342.0	**0.36**
	2%	158.6	342.0	**0.46**
	3%	201.3	342.0	**0.59**
	4%	231.4	342.0	**0.68**
	-0.5%	117.9	342.0	**0.34**
	-1%	148.3	342.0	**0.43**
	-2%	163.9	342.0	**0.48**
	-3%	171.0	342.0	**0.50**
	-4%	173.3	342.0	**0.51**
SB-LA	0.5%	70.5	557.3	**0.13**
	1%	131.5	557.3	**0.24**
	2%	190.8	557.3	**0.34**
	3%	226.7	557.3	**0.41**
	4%	236.8	557.3	**0.42**
	-0.5%	109.0	557.3	**0.20**
	-1%	146.9	557.3	**0.26**
	-2%	181.2	557.3	**0.33**
	-3%	179.2	557.3	**0.32**
	-4%	192.2	557.3	**0.34**

It can be seen from **Figure 14** that, the beam contacted the column through entire beam section at neutral position. At peak drift angle position, contacted area limited only on small areas at the top or bottom of the beam. After several cycles, the concrete and grout at these areas was crush and softened, causing the deterioration of friction coefficient. Similar results were found in the study by Okamoto[8]. It can be concluded that the contribution of shear friction mechanism to the shear strength of the connection decreased when the drift angle increased, especially at peak drift angle position.

4. Conclusions

From results of this study, following conclusions can be drawn.

1) Modified shear bracket and beam socket worked well to transfer the shear force from the beam to the column, as well as satisfy the deformability of the beam at high level of drift.

2) The specimens with shear bracket expressed very good seismic performance, with small residual deformation, fully developed and column element, even in very long span frame. It is high possibility to apply this type of connection in real precast building structures.

3) The specimens without shear bracket experienced large beam slip and residual deformation. The slip occurred at the friction coefficient of 0.45. Performance of the system without bracket was inferior compares to the system with shear bracket.

4) The slip of the beam was the cause of the

difference of flexural strength between positive and negative direction.

5) At small drift angle, most of shear strength of the connection was contributed by shear friction mechanism. When the drift angle increased, contribution of shear friction decreased and that of the shear bracket increased.

REFERENCES

[1] Đỗ Tiến Thịnh (2009), Luận án Tiến sĩ kỹ thuật, *Đại học Quốc gia Yohohama.*

[2] Đỗ Tiến Thịnh, Koichi Kusunoki, Akira Tasai (2008), Study on A New Precast Post-Tensioned Beam-Column Joint System", *Tạp chí Khoa học Công nghệ Xây dựng, số 4, trang 25-31.*

[3] Architecture Institute of Japan (2003), "Standard for Structural Design and Construction of Precast Concrete Structures", *in Japanese.*

[4] Architecture Institute of Japan, "Standard for Structural Design and Construction of Prestressed Concrete Structures", *1998, in Japanese.*

[5] Prestressed Concrete Institute, "PCI Design Handbook", *6th Edition, 2004.*

[6] S. Pampanin (2005), "Emerging Solution for High Seismic Performance of Precast/Prestressed Concrete Buildings", *Journal of Advanced Concrete Technology, Vol. 03, No. 02, June, pp 207-223.*

[7] I. Kawakubo, T. Ishioka, T. Nishimura, Y. Hosoi, N. Aragane, M. Kanagawa, S. Takeda (2008), "Development of a Large-Span Precast Concrete Structural System with Ease of Construction Using Prestressed Connections, Part 10 Verification by Dynamic Response Analysis (1)", *Proceedings of Architecture Institute of Japan Annual Convention, September, pp 669-670.*

[8] H. Okamoto, and T. Hirade (1997), "Shear transfer on the beam-column prestressed joint under earthquake loads: Relation between the maximum experienced deformation and the loss of prestressing force/the deterioration of the shear strength", *Proceedings of Architecture Institute of Japan Annual Convention, September, pp 901-902.*

Ngày nhận bài:*23/8/2017.*

Ngày nhận bài sửa lần cuối: *06/9/2017.*